25) *Trautman, R.*, Biochim. Biophys. Acta **28**, 417 (1958).
26a) *Edsall, J. T.* in: The Proteins (Ed. *H. Neurath K. Bailey*) p. 722 (New York 1953). b) *C. B. Anfinsen* und *R. R. Redfield* in: Advances in Protein Chemistry, Vol. XI, p. 62 (New York 1956).
27) *Strauss, U. P.* und *R. M. Fuoss* in: *H. A. Stuart*, Physik der Hochpolymeren, Bd. 2, S. 680ff. (Berlin–Göttingen–Heidelberg 1953).
28) *Kirkwood, J. G.* und *J. Riseman*, J. Chem. Phys. **16**, 565 (1948).
29) *Mandelkern, L.* und *P. J. Flory*, J. Chem. Phys. **20**, 212 (1952).
30) *Tanford, C.*, J. Amer. Chem. Soc. **72**, 441 (1950).
31) *Stauff, J.* (unveröffentlicht).
32) *Stauff, J.*, Kolloidchemie, S. 612f. (Berlin–Göttingen–Heidelberg 1960).
33a) *Yang, J. T.* und *J. F. Foster*, J. Amer. Chem. Soc. **76**, 1588 (1954). b) *C. Tanford* und *J. G. Buzzell*, J. Phys. Chem. **60**, 225 (1956).
34) *Djerassi, C.*, Optical Rotatory Dispersion, (New York 1960).
35) *Kauzmann, W.* in: Advances in Protein Chemistry, Vol. XIV, p. 1 (New York 1959).
36) *Blout, E. R.* in: Proc. IVth International Congress of Biochemistry 1958, Vol. IX, p. 37 (London 1959).
37) *Šorm, F.* in: Symp. Protein Structure 1957, (*Ed. A. Neuberger*), p. 79 (London, New York 1958).

From the Institute of General Chemistry, Department of Technical Physics, Warszawa 27 (Poland)) and the Synthetic Fibres Factory, Physico-Chemical Laboratory, Gorzów Wlkp. (Poland)*

Mechanical Aspects of Fibre Spinning Process in Molten Polymers

Part III.: Tensile Force and Stress

By Andrzej Ziabicki

With 16 figures in 19 details and 2 tables

(Received August 23, 1960)

Introduction

In the former papers concerning the mechanics of fibre spinning (1,2) the process was considered from the kinematical point of view. The tensile force F was not precisely defined nor estimated. It is the purpose of this paper to give a theoretical analysis of force and stress constituents in the fibre spinning process and to compare them with experimental results found for melt-spun polyamide fibres.

Theoretical

Considering the fibre forming material (polymer-melt or solution) as a liquid, the general hydrodynamical equations for motion may be written:

$$f_x - \frac{\partial P}{\partial x} + \eta \nabla^2 V_x = \varrho \left[\frac{\partial V_x}{\partial t} + V_x \frac{\partial V_x}{\partial x} + V_y \frac{\partial V_x}{\partial y} + V_z \frac{\partial V_x}{\partial z}\right] \quad [1a]$$

$$f_y - \frac{\partial P}{\partial y} + \eta \nabla^2 V_y = \varrho \left[\frac{\partial V_y}{\partial t} + V_x \frac{\partial V_y}{\partial x} + V_y \frac{\partial V_y}{\partial y} + V_z \frac{\partial V_y}{\partial z}\right] \quad [1b]$$

$$f_z - \frac{\partial P}{\partial z} + \eta \nabla^2 V_z = \varrho \left[\frac{\partial V_z}{\partial t} + V_x \frac{\partial V_z}{\partial x} + V_y \frac{\partial V_z}{\partial y} + V_z \frac{\partial V_z}{\partial z}\right]. \quad [1c]$$

For free liquid stream, not limited by any vessel walls we have:

$$P = 0 .$$

The considered process is assumed to be continuous and steady and the velocity field is assumed to have no constituents but V_{xx} [1])

$$\partial V_x/\partial t = 0; \quad V_y = V_z = 0; \quad \partial V_x/\partial y = \partial V_x/\partial z = 0 .$$

With above conditions the equation [1a] may be written as follows:

$$f_x + \eta \left(d^2 V_x/dx^2\right) - \varrho V_x \left(\partial V_x/\partial x\right) = 0 . \quad [2]$$

The variable x is a distance from spinneret measured along the stream (spinning way l in former papers) (see fig. 1).

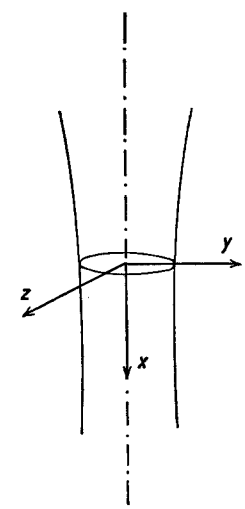

Fig. 1. Vide text

*) Address for correspondence.

[1]) The validity of this assumption will be discussed in the next section.

In eq. [2] the force density f_x is composed of several constituents which will be discussed below. The term: $\eta \cdot \nabla^2 V_x$ [or: $\eta (\partial^2 V_x/\partial x^2)$ in the conditions assumed] is a force density arising from the internal friction of newtonian liquid. In our problem the considered macromolecular liquids are non-newtonian in general. Hence it seems to be more correct to replace the term: $\eta \cdot \nabla^2 V_x$ by a general expression f_{rheo} (the density of rheological force) which describes the drag of internal friction. In the particular case when the liquid is newtonian it is:

$$f_{\text{rheo}} = \eta \cdot \nabla^2 V_x .$$

The term: $\varrho V_x \cdot (\partial V_x/\partial x)$ describes the force density due to inertia. The eq. [2] in its final form may be written:

$$f_x + f_{\text{rheo}} - \varrho V_x \cdot (\partial V_x/\partial x) = 0 . \qquad [2a]$$

In the above equations the symbol f determines the density of tensile force in a given point of liquid stream $f_x = dF_x/dv$, and F determines the force acting on the whole stream on the distance x from spinneret.

The constituents of force F

In eq. [2a] besides the above explained rheological and inertial terms there is a complex force density expression f_x composed of 3 constituents. In the following treatment the force constituents directed conformably to velocity will be taken positive, those directed oppositely to velocity–negative.

The force density f_x consists of:

force of gravity ($f_{\text{grav}} = \varrho g$, positive)

aerodynamical drag of polymer stream (fibre) running in a gaseous medium (f_{aero}, negative)

force arising from the surface tension of polymer liquid (f_{surf}, negative).

Assuming the force density distribution to be uniform through the stream cross-section:

$$\partial f/\partial y = \partial f/\partial z = 0$$

eq. [2a] may be multiplied by the area of cross-section A and the expressions of force density replaced by force gradients along the spinning way: $f \cdot A = dF/dx$. Considering additionally the equation of continuity:

$$\varrho V \cdot A = \text{const.} = W , \qquad [3]$$

it may be finally written:

$$\varrho g A - \frac{dF_{\text{aero}}}{dx} - \frac{dF_{\text{surf}}}{dx} + \frac{dF_{\text{rheo}}}{dx} - W\frac{dV_x}{dx} = 0 . \qquad [4]$$

The gravitational constituent of tensile force

The weight of the hanging fibre:

$$F_{\text{grav}} = \int_x^L \varrho g A \, dx \qquad [5]$$

should be taken into account when thick fibres are spun. For thin fibres the gravitational force (an integral of ϱgA in the limits from x to the end of spinning way L) makes only a small part of the whole force needed for fibre formation. The force F_{grav} has its maximal value at the beginning of the spinning way ($x = 0$) and monotonically decreases to zero at the end of the spinning way ($x = L$).

If we assume, in the first approximation, the stream (fibre) to have on the whole way the same final thickness, the gravitational force results in amount of about 10^{-3} dynes/1 denier · 1 cm of the spinning way.

The aerodynamical constituent results from an external friction of running stream (fibre) in the surrounding medium. According to the principles of aerodynamics the force dF_{aero} resulting from the friction of surface $\pi d \cdot dx$ moving with a velocity V in gas of density ϱ amounts to:

$$dF_{\text{aero}} = (\varrho V^2/2)\, \pi d \cdot dx \cdot C(Re) , \qquad [6]$$

where Re is a *Reynolds* number:

$$Re = \frac{V \cdot L}{\nu} .$$

There are no drag coefficients $C(Re)$ given in the literature for wires or thin fibres running axially in gaseous medium as required in our problem. As an approximation the coefficients of *Prandtl* (3) for flat plate have been applied, as have done other authors investigating the spinning of cellulose fibres (4, 5).

$$C(Re) = 1.327\, Re^{-0.5} \text{ for laminar motion} \qquad [7a]$$

$$C(Re) = 0.074\, Re^{-0.2} \text{ for turbulent motion} \qquad [7b]$$

Putting in eqs. [6, 7a, and 7b] the parameters of an air, the formulas for force gradient result:

$$dF_{\text{aero}}/dx = 9.77 \times 10^{-4}\, d \cdot L^{-0.5}\, V^{1.5} \qquad [7c]$$

for laminar motion

$$dF_{\text{aero}}/dx = 0.98 \times 10^{-4}\, d \cdot L^{-0.2}\, V^{1.8} \qquad [7d]$$

for turbulent motion.

In the conditions usually applied in technological practice, e. g. $L = 450$ cm and $V = 300$–3000 m/min, the *Reynolds* numbers are of the order 10^6–10^7 (transition region). For the estimation of maximal values of F_{aero} in this section the formula [7d] was

used. For the calculation of F_{aero} in the spinning experiments carried out with rather low velocity the formula [7c] was used.

From the above formulas it may be seen that the aerodynamical force strongly increases with fibre velocity V. For the conditions occurring in practice, e. g. for a bundle of 12 fibres each of diameter 0.005 cm, 450 cm long, running with a velocity V = 1000 m/min, F_{aero} amounts to 490 dynes, and makes several percents of the whole drawing force.

The force F_{aero} for any distance x from spinneret should be calculated as an integral of force gradient in the limits from x to L

$$F_{aero} = \text{const.} \int_x^L d \cdot L^{-a} V^{2-a} dx , \qquad [7e]$$

where $a = 0.5$ and 0.2 for laminar and turbulent motions respectively.

Like F_{grav}, the aerodynamical force has its maximal value at $x = 0$ and decreases to zero at $x = L$.

The constituent F_{aero} is much more important in the case of spinning fibres after the "wet-spinning" procedure. The friction in the viscous liquid bath may be some orders greater than that in an air and is one of the limitations for take-up velocity.

The surface tension of fibre-forming liquid is connected with a force F_{surf}, which tends the liquid stream to shrink and to increase its diameter. Hence it is directed oppositely to the velocity and negative in our treatment.

On the distance x from spinneret, where the stream has a diameter d the force F_{surf} amounts to:

$$F_{surf} = \pi d \cdot \mu , \qquad [8]$$

where μ = surface tension.

It may be assumed that the surface tension of a macromolecular, fibre-forming liquid is not greater than that of simple organic liquids of similar constitution. Putting e. g. μ = 50 dynes/cm, F_{surf} results in amount of 50 dynes per 1 cm of fibre perimeter. The maximal values of F_{surf} occur at $x = 0$, where $d = d_0$ – the diameter of spinneret channel.

E. g. for the 12-filaments-yarn spun of a spinneret with channels d_0 = 0,025 cm, the maximal F_{surf} will be of the order of 47 dynes. It is so small as compared with other constituents, that it may be completely neglected in calculations.

In the spinning of fibres of very fluid liquid, the surface tension may come into consideration as a factor tending to split the stream into single drops.

The inertial term F_{inert} – is a force needed to the acceleration of polymer mass from a given velocity V to the final, take-up velocity V_E. This force is, of course, directed oppositely to velocity, hence negative in our treatment.

In the continuous stream:

$$dF_{inert}/dx = W \cdot dV/dx \qquad [9a]$$

and

$$F_{inert,\,x} = W (V_E - V_x) . \qquad [9b]$$

The maximal value occurs at $x = 0$ and amounts to $W \cdot (V_E - V_0)$. F_{inert} monotonically decreases along the spinning way till to $x = l_\infty$ where it becomes zero. Dependently on flow intensity W and take-up velocity V_E, F_{inert} in practice may amount to 10–10^3 dynes.

The rheological force F_{rheo} – is a substantial part of drags connected with fibre formation. F_{rheo} varies along the spinning way according to rheological behaviour of polymer stream, its cross-section, and velocity gradient G. Considering the deformation of polymer stream as a viscous or plastic traction with variable coefficients of viscosity λ (1) the local rheological force $F_{rheo,\,x}$ is given by relations:

$$F_{rheo,\,x} = A \cdot \lambda (x) \cdot \frac{dV}{dx} \qquad [10a]$$

for viscous traction

and

$$F_{rheo,\,x} = A \left[\sigma_y (x) + \lambda (x) \cdot \frac{dV}{dx} \right] \qquad [10b]$$

for plastic traction with a variable yield stress σ_y.

The eqs. [10a] and [10b] comprise the unknown functions $\lambda(x)$ and $\sigma_y(x)$ – the distributions of apparent *Trouton* viscosity and yield stress along the spinning way. Therefore the calculation of F_{rheo}, even when the stream profile is known

$$\left[A (x), \text{ and } \frac{dV}{dx} (x) \right],$$

cannot be accomplished. Instead of it, the force F_{rheo} may be determined from the balance of forces as shown below.

The eq. [4] multiplied by an infinitely short element of spinning way dx, with neglecting the constituent F_{surf} may be written:

$$\varrho g \cdot A \, dx - \text{const}\, d \cdot V^2 C(Re) \cdot dx + dF_{rheo} - W \cdot dV = 0 \qquad [11]$$

and after integration in the limits x, L:

$$\int_x^L \varrho g \cdot A \, dx - \text{const} \int_x^L d \cdot V^2 C(Re) \, dx + F_{rheo,\,L} - F_{rheo,\,x} - W (V_E - V_x) = 0 . \qquad [12]$$

Besides it is known, that at the end of spinning way ($x = L$) the rheological force $F_{\text{rheo},L}$ is equal to the external, take-up force F_{ext} produced by the winding drum of the take-up device:

$$F_{\text{rheo},L} = F_{\text{ext}} . \qquad [13]$$

The last one can be easily measured with a tensometer at the end of spinning way.

Putting F_{ext} in the eq. [12] we obtain:

$$F_{\text{rheo},x} = F_{\text{ext}} + \int_x^L \varrho\, g\, A\, dx - \text{const} \int_x^L d \cdot V^2 C(Re)\, dx - W\,(V_E - V_x) \qquad [14a]$$

or in other symbols:

$$F_{\text{rheo},x} = F_{\text{ext}} + F_{\text{grav},x} - F_{\text{aero},x} - F_{\text{inert},x} . \qquad [14b]$$

Basing on these formulas, the rheological force, very important for the spinning process, will be calculated in further sections.

The external force F_{ext} – appeared in eq. [14] from the limiting condition [13]. This constituent should be meant as a difference between the sum of drags connected with spinning (sum of negative constituents: rheological, aerodynamical, inertial) and the gravitational force.

When the fibre being spun is rather thick and low viscous, the *additional* force F_{ext} needed to *cooperate* with the gravity in the balancing of drags is small. In some cases the gravitational force may be strong enough to surmount all the drags; then $F_{\text{ext}} = 0$ and we have to do with so-called "gravitational spinning" i. e. with a drawing of stream upon its own weight. The condition for gravitational spinning is:

$$F_{\text{ext}} = 0 \qquad [15a]$$

or

$$F_{\text{grav}} = F_{\text{rheo}} + F_{\text{aero}} + F_{\text{inert}} . \qquad [15b]$$

When $F_{\text{ext}} = 0$ the normal spinning is not possible. The fibre cannot be wound on the drum or bobbin and it makes an appearance if the fibre was not solidified and "flew" as a liquid. The substantial origin of this effect, however, is not "fluidity" of polymer but the lack of external force and stress.

In the case of spinning thin fibres with high viscosities, the sum of drags is much greater than the gravitational force F_{grav} and so is the external force F_{ext}. In most cases in practice the gravitational force is negligible small as compared with F_{ext}. Then:

$$F_{\text{grav}} \ll F_{\text{ext}} \qquad [16a]$$

and

$$F_{\text{ext}} \approx F_{\text{rheo}} + F_{\text{aero}} + F_{\text{inert}} . \qquad [16b]$$

Since F_{ext} is constant on the whole spinning way, in the case described by eq. [16b] the sum of drags is also constant along the way. In other words, the profile of stream and the distribution of diameter, velocity and velocity gradient must be so, that in every point x the sum of drags is constant.

On the contrary, in the first case ($F_{\text{ext}} = 0$) the drawing force, as well as the sum of drags, continuously decreased along the way. From the technical point of view the spinning with higher external forces and constant sum of drags seems to be more steady and to give more even fibres.

The problem of transverse (radial) velocity gradient

The above treatment was based upon the assumption, that the distributions of force, velocity and viscosity were uniform through the stream cross-section. In the following considerations this assumption will be discussed, and consequences are analyzed arising from the radial distribution of polymer viscosity. In the following treatment the hydrodynamical equation will be written in cylindrical coordinates with a condition of symmetry:

$$\partial(f, V, \lambda)/\partial\varphi = 0 .$$

Two problems will be discussed separately:

1. The radial velocity distribution in the region placed immediately below the spinneret ("region of equalization").
2. The radial distribution of viscosity, velocity and stress in the farther region, where the conditions of flow in the channel of spinneret do not play any important role ("steady region").

The distribution of stream velocity in the "region of equalization"

The profile of velocity of a viscous liquid flowing through a capillary is parabolic. Such a distribution of velocity is assumed to occur in the channel of spinneret[2]). In the moment when the liquid leaves the spinneret ($x = 0$) disappears the origin of radial velocity distribution: the friction of outer layers on the walls of channel is zero. The process of laminar motion begins to turn: the fast running central layers are now braked by slower peripherical ones, what

[2]) When very short channels are applied, the normal, parabolic profile of velocity cannot be realized; the perfection of velocity distribution within the spinneret channel, however, is quite another problem.

leads to an equalization of velocity through the stream cross-section (fig. 2a). The flow of a viscoelastic, fibre-forming liquid in the short channel of spinneret is accompanied by the effect of stream-broadening and decreasing of average stream velocity (2). That effect results from the relaxation of residual internal stress and, probably, of the disorientation of macromolecules, oriented in the channel. When a definite point of maximal broadening is passed (what evidently corresponds to the complete relaxation and disorientation) begins the process of drawing and increasing the average stream velocity (fig. 2b).

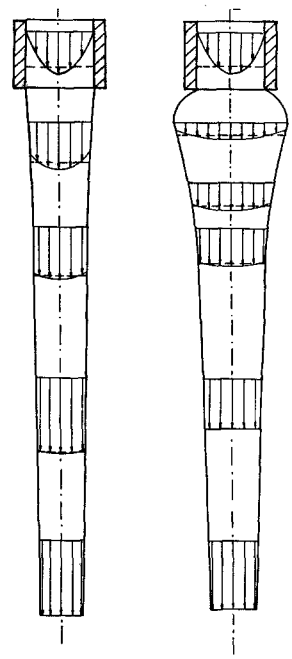

a) b)

Fig. 2. Profiles of stream velocity in the "region of equalization". a) without stream broadening – b) with a stream broadening

It seems to be evident, that the decrease of average velocity in the region of broadening shortens the process of equalization. It may be supposed in normal spinning, that the zone of equalization is of the same order as the zone of broadening, i. e. several millimeters or centimeters. Such processes seem to play no important role in the forming of fibre structure and properties.

The distribution of velocity, viscosity and stress in the "steady region"

In the region, where the spinneret has no influence on the flow, there are two possible origins of deviation from the uniform radial distribution of velocity and stress:

a) the surface forces

b) the radial viscosity gradient.

Amongst the above considered force constituents, there are two acting on the surface of stream only: the aerodynamical drag, and the surface tension. Let us consider the first of them.

Assume, that on the surface of an infinitely short segment dx of stream with diameter d acts force dF_{aero}. The deformation of stream resulting from that action is similar to that occurring in the capillary, while the peripherical layers are braked and slide respectively the central ones.

The maximal tangential stress amounts to:

$$p_{\max} = \frac{dF_{\text{aero}}}{\pi d \cdot dx} \qquad [17\text{a}]$$

and the corresponding maximal transverse velocity gradient:

$$D_{\max} = [\partial V/\partial r]_{\max} = \frac{1}{\pi d \cdot \eta} \frac{dF_{\text{aero}}}{dx} . \qquad [17\text{b}]$$

Substituting in the eq. [17b] the values of dF_{aero}/dx from eq. [7c, d] it results:

$$D_{\max} = 3{,}11 \times 10^{-4} L^{-0.5} V^{1.5} \eta^{-1} \qquad [18\text{a}]$$

for laminar motion

and

$$D_{\max} = 0{,}312 \times 10^{-4} L^{-0.2} V^{1.8} \eta^{-1} \qquad [18\text{b}]$$

for turbulent motion.

For the maximal take-up velocities of the order 3000 m/min and minimal stream viscosity $\eta = 1000$ poises the maximal gradient $D_{\max}$ amounts to $10^{-2} - 10^{-3}$ sec^{-1}. The transverse velocity gradients within the channel of spinneret are of the order 10^3–10^5 sec^{-1}, and the parallel velocity gradients occurring in the spinning process of the order 1,0–10^2 sec^{-1}. Hence the effects arising from the surface forces are negligibly small and do not play any important role in the process of spinning. The forces, and the transverse velocity gradients connected with surface tension are even smaller.

Only by wet-spinning, where we have to do with a friction in a liquid, viscous bath, the effects arising from the surface forces may be stronger pronounced.

The radial distribution of viscosity

In the fibre spinning from molten polymers there is always some radial temperature gradient, connected with a gradient of viscosity:

$$(\partial\lambda/\partial r) = \left(\frac{d\lambda}{dT}\right) \cdot \left(\frac{\partial T}{\partial r}\right). \qquad [19]$$

Considering the cooling of polymer stream as an unsteady process of heat transfer, the radial temperature gradient may be expressed as a function of *Biot* number Bi, stream radius R, the distance from the stream axis r and the temperature on the axis ($r = 0$), referred to the temperature of surroundings Θ_0 (6):

$$(\partial T/\partial r) = f(Bi, R, r, \Theta_0)\,. \qquad [20]$$

The starting point for the calculations is the *Heisler*'s diagram of the relation:

$$(\Theta_s/\Theta_0) = \Phi(s, Bi)\,, \qquad [21]$$

where: $s = r/R$ — relative distance from stream axis

$\Theta_s = T_s - T_{surr}$ = the temperature on the distance s referred to the temperature of surroundings T_{surr}

$\Theta_0 = T_0 - T_{surr}$ = the temperature on the axis ($s = 0$) referred to the temperature of surroundings.

Bi = *Biot* number.

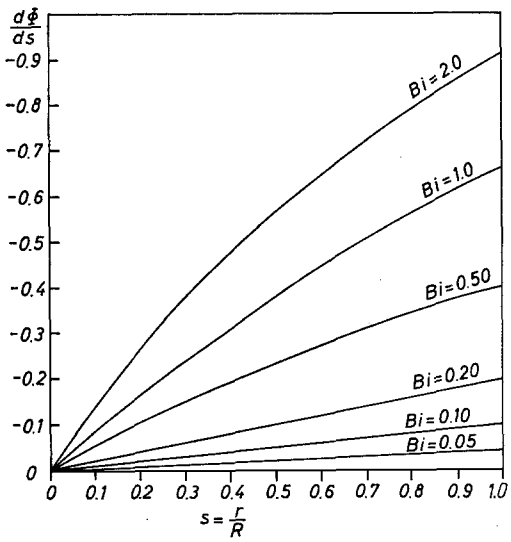

Fig. 3. Function $[d\Phi/ds]_{Bi}$ versus $s = r/R$

In the fig. 3 there is shown the diagram of function $(d\Phi/ds)_{Bi}$, vs. s as obtained from transformation and differentiation of *Heisler*'s diagram. It may be easily shown, that the radial temperature gradient is related to function $(d\Phi/ds)$ by equation:

$$[\partial T/\partial r]_{Bi,R,r,\Theta_0} = \frac{\Theta_0}{R} \cdot \frac{d\Phi}{ds}(Bi, s = r/R)\,. \qquad [22]$$

The temperature gradient has maximal values in the initial region of cooling (high Θ_0/R ratios) and decreases along the spinning way.

The temperature variation of polymer viscosity may be approximately described by *Eyring-Frenkel* equation:

$$\lambda = A \cdot \exp(E/RT) \qquad [23]$$

hence

$$d\lambda/dT = -EA/RT^2 \cdot \exp(E/RT) = -E/RT^2 \cdot \lambda\,. \qquad [24]$$

The absolute values of $d\lambda/dT$ increase with decreasing temperature along the spinning way.

In order to estimate the order of magnitude of the maximal radial viscosity gradients occurring in the process of spinning, the conditions on the initial part of the spinning way were considered.

Assume the activation energy of flow $E = 15000$ cal/mole, an absolute temperature $T_0 = 523°$ K and corresponding *Trouton* viscosity $\lambda = 6000$ poises.

The decrease of viscosity per 1° K results from eq. [24]:

$$d\lambda/dT \approx 166 \text{ poises/° K}\,.$$

Assuming fibre radius to be $R = 0.005$ cm, $\Theta_0 = 523 - 298 = 225°$ K, and $Bi = 0.1$ the maximal temperature gradient (on stream surface, $s = 1$) results from eq. [22] with an aid of fig. 3:

$$[d\Phi/ds]_{s=1, Bi=0.1} = 0.105$$

$$[\partial T/\partial r]_{max} \approx 1180° \text{ K/cm}$$

and the maximal viscosity gradient:

$$[\partial\lambda/\partial r]_{max} \approx 1{,}96 \times 10^5 \text{ poises/cm}\,.$$

Similar, or even greater viscosity gradients along the stream radius may be expected in other spinning procedures. In the spinning after "dry-method" the viscosity gradient is connected with a gradient of polymer concentration:

$$[\partial\lambda/\partial r] = \left(\frac{d\lambda}{dc}\right) \cdot \left(\frac{\partial c}{\partial r}\right). \qquad [25]$$

In the spinning after the "wet–method" in a precipitation bath this effect is more complicated because of the coagulation and precipitation of polymer from the solution. Viscosity gradients in "wet-spinning" are probably much greater than those occurring in the melt-or dry-spinning; there is a rigid, outer layer of precipitated polymer, "skin", distinctly separated from the inner, fluid "core".

The "skin-effects" in melt-spinning, if occurring, are only slightly pronounced.

The consequences of the occurrence of radial viscosity gradient

By the non-uniform radial distribution of viscosity, the hydrodynamic equation [1 a]

should be written in form:

$$f_x + \eta(x,r)\left[\frac{\partial^2 V_x}{\partial x^2} + \frac{\partial^2 V_x}{\partial r^2} + \frac{1}{r}\frac{\partial V_x}{\partial r}\right] - \varrho\frac{\partial V_x}{\partial x} V_x = 0\,. \qquad [26]$$

The solution of eq. [26] is rather difficult to obtain. In the present paper only some special cases will be qualitatively discussed.

A non-uniform radial distribution of viscosity excludes the possibility of simultaneously occurring of uniform velocity- and stress-distribution. Two particular cases will be discussed below:

1. uniform stress distribution: $\partial\sigma/\partial r = 0$
2. uniform velocity distribution: $\partial V/dr = 0$

1. Assume that the only force acting on the liquid stream in the direction x is gravity. The condition:

$$\partial f_x/\partial r = 0$$

is automatically fulfilled, and the tensile stress calculated on the area of stream cross-section is constant.

Consider a short, cylindrical segment of stream, consisting of concentrical layers of different, increasing from axis to surface, viscosity (fig. 4).

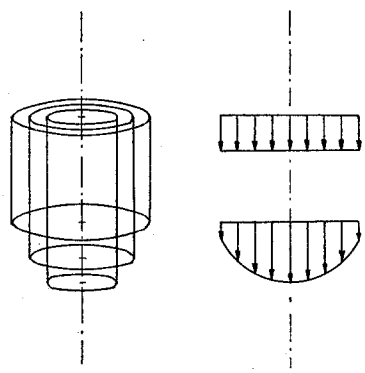

Fig. 4. Model of stream deformation at uniform stress distribution and a radial viscosity gradient; left: stream, right: velocity distribution

Every layer of thickness dr undergoes an action of force

$$dF = 2\pi r \cdot dr\,\sigma\,.$$

When constant stress σ is applied, the velocity gradients G resulting in various layers are different:

$$G(r) = [\partial V/\partial r]\,(r) = \frac{\sigma}{\lambda} \qquad [27]$$

and for

$$\partial\lambda/\partial r > 0; \quad \partial G/\partial r < 0\,.$$

The central layers of less viscosity will be stronger deformed than the more viscous peripherical ones. It leads to the mutual sliding of the layers – to the *shearing*.

The force dF acting on the element of cross-section $dA = 2\pi r \cdot dr$ will be distributed between the viscous traction and shearing:

$$dF = 2\pi r \cdot dr \cdot \sigma = 2\pi r \cdot dr \cdot \lambda(r)\,G(r) + 2\pi r \cdot dx \cdot \eta(r)\,D(r) \quad [28a]$$

or:

$$dF/dr = 2\pi r\left[\lambda(r)\frac{\partial V_x}{\partial x}\,dr + \eta(r)\frac{\partial V_x}{\partial r}\,dx\right]. \quad [28b]$$

It is evident from this simplified model, that the deformation comprises both traction and shearing; besides the parallel velocity gradient G and *Trouton* viscosity λ appear the transverse velocity gradient D and newtonian viscosity. The assumed condition of constant stress which leads to an appearance of transverse velocity gradient can be accomplished only in some special cases: e. g. by infinitely slow (without acceleration) gravitational spinning. The technical spinning process is very far from such conditions. In technology, however, the second case is more important: the uniform velocity distribution.

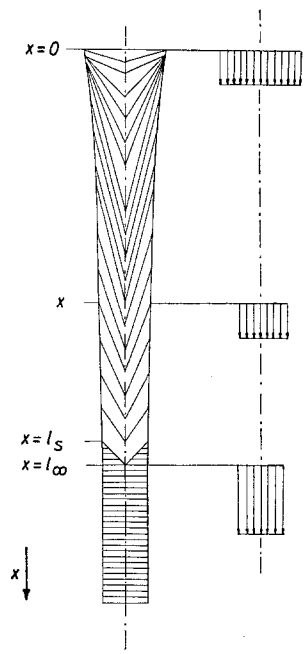

Fig. 5. Model of stream deformation at uniform velocity distribution and a radial viscosity gradient; left: stream, right: velocity distribution

2. Consider the model shown in fig. 5. An axially symmetrical stream consists of thin conical layers of different viscosity. The dashed area determines the solid body which does not undergo deformation in given conditions.

At the distance $x = l_\infty$ the fibre is completely solidified, has a constant diameter d_E, and velocity V_E. The distance l_s determines the beginning of an appearing of solid layer, which gradually grows to $x = l_\infty$.

In the region of solid fibre ($x \geq l_\infty$) the velocity is constant through the cross-section and amounts in every point to V_E. At the beginning of the spinning way ($x = 0$) the velocity is also constant through stream cross-section (for $x = 0$ is assumed here the "point of equalization" below the spinneret).

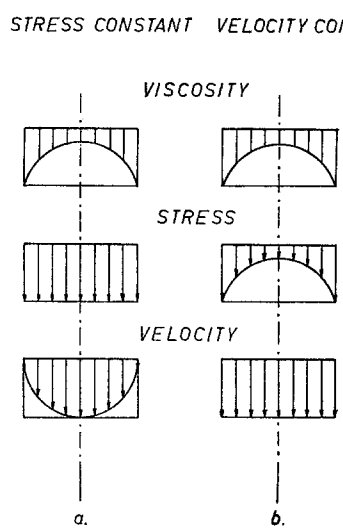

Fig. 6. Scheme of viscosity, stress and velocity distributions. a. stress distribution uniform – b. velocity distribution uniform

Hence, if the condition of continuity is to be fulfilled, in every stream cross-section placed on any distance x from spinneret the velocity V_x must be constant on the stream radius: $\partial V_x/\partial r = 0$. In order to obtain equal deformations in layers of different viscosities a non-uniform distribution of stress is needed.

It was shown, that the uniform distribution of stress brings about a non-uniform distribution of velocity; the uniform distribution of velocity brings about a non-uniform distribution of stress. Those distributions in both cases are schematically drawn in fig. 6. The occurring of different viscosities and stresses at equal deformations in various layers causes a different orientation of macromolecules on various fibre radius [cf. mechanism of orientation (7, 8)]. The more viscous peripherical layers will be more oriented, the central, less viscous ones – less oriented. The radial distribution of viscosity is in fibre spinning process connected with a radial distribution of orientation and with "skin effects".

The forming of a solid layer on the surface of stream ("skin") is especially important in the "wet-spinning" procedure. In the region of "growing skin" ($|l_s, l_\infty|$ in fig. 6) the thin, solid skin transfers the most part of the drawing force. It leads to the strong orientation of the macromolecules in the "skin" on one hand, and makes limits for deformation- and precipitation rates on another one. Similar, but more slightly expressed effects may be expected also in other spinning procedures.

Experimental

The purpose of experiments carried out on polycapronamide fibres was:

1. to determine the external (take-up) force F_{ext} and to calculate the distribution of force constituents, stress and apparent viscosity along the spinning way.
2. To investigate the influence of spinning conditions upon the take-up force, rheological force and stress.

The material (polycapronamide), apparatus, and methods of spinning were described in the first paper (1).

The measurements of force F_{ext} were carried out with an electronic, recording tensiometer TENSOTRON (*f-ma Zimmer*) equipped with measuring heads 10 G and 30 G. The measurements of force F_{ext} were accomplished immediately before the first winding drum

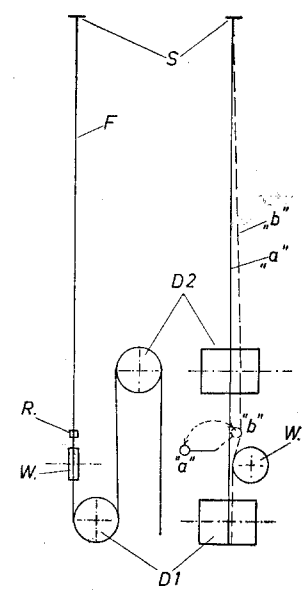

Fig. 7. Scheme of fibre leading system. S – spinneret, F – stream (fibre), D_1, D_2 – winding drums, W – wetting disc, R – leading roll, B – bobbin; position "a" (solid line) – freely running fibre; position "b" (dotted line) – fibre led through the wetting device

D 1 by free-running fibre, without leading through the wetting device or any other drags (see fig. 7, position "*a*"). The measurements of force in technical conditions (fig. 7 position "*b*") were carried out in separate experiments.

Some typical force diagrams as obtained from tensiometer are shown in fig. 16. In the calculations of stress and viscosity the data of stream cross-section A, and velocity gradient G were taken from the first paper (1)

Results and Discussion

The distribution of tensile force, stress and apparent viscosity along the spinning way

In the figs. 8 and 9 the distribution of individual force constituents along the way is shown for two monofilaments:

A 5. gravitational spinning
($F_{ext} = 0$), $Td = 124$ drs; $V_E = 210$ m/min; $L = 450$ cm

A 8. normal spinning
($F_{ext} \neq 0$), $Td = 40$ drs; $V_E = 656$ m/min; $L = 450$ cm.

In the diagrams presented by figs. 8 and 9 the take-up force F_{ext} is a result of direct measurements; the constituents F_{grav}, F_{aero}, F_{inert}, and F_{rheo} were calculated point by point according to formulas [5, 7e, 8, 9b, 14a]. The positive constituents (F_{ext} and F_{grav}) were plotted above, the negative ones (drags): F_{aero}, F_{inert} and F_{rheo}, below the x-axis.

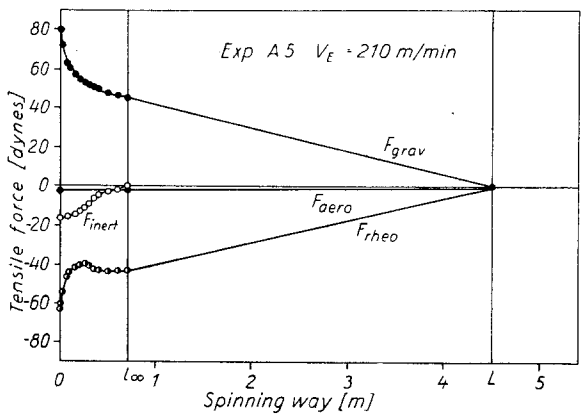

Fig. 8. Distribution of force constituents along the spinning way. Experiment No. A5

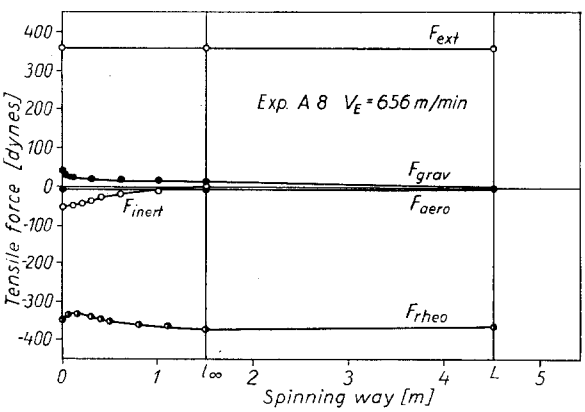

Fig. 9. Distribution of force constituents along the spinning way. Experiment No. A8

It is evident from fig. 8 that in the gravitational spinning the only positive constituent (F_{grav}) strongly decreases along the spinning way. This leads to a similar decrease of rheological force F_{rheo} which makes about 80% sum of drags. Over the distance l_∞ both F_{grav} and F_{rheo} linearily fall to zero at $x = L$.

When a rather thin monofilament is spun (fig. 9) the total drawing force (sum of positive constituents) consists of a constant F_{ext} and a variable F_{grav}. The last one is small as compared with F_{ext} and in its maximal point ($x = 0$) does not exceed 10,3% $F_{tot} = F_{ext} + F_{grav}$. The rheological force F_{rheo} makes about 86,5% sum of drags and is more constant on the way than by gravitational spinning. The extrema visible on the F_{rheo}-curve are connected with variation of other constituents. The force F_{aero}, at given velocities and diameters not exceeding 1–5 dynes, i. e. 1–3% sum of drags, falls in the region 0, l_∞ curvilinearily, and in the region l_∞, L linearily along the way. The force F_{inert}, proportional to the velocity difference, has an inflexion point, corresponding to the maximum of velocity gradient ($x = l_c$) and falls to zero at $x = l_\infty$. The maximal values of F_{inert} do not exceed 12–22% sum of drags.

In the figures 10, 11, 12 there are shown the distributions of stress $\sigma = F_{rheo}/A$, and apparent *Trouton* viscosity $\lambda_a = \sigma/G$ for three spinning experiments described in the first paper (1):

A 5. gravitational spinning,
$Td = 124$ drs; $V_E = 210$ m/min; $L = 450$ cm

A 19. normal spinning,
$Td = 68$ drs; $V_E = 381$ m/min; $L = 450$ cm

A 8. normal spinning,
$Td = 40$ drs; $V_E = 656$ m/min; $L = 450$ cm.

For each experiment the stress has a maximum placed at the point $x = l_\infty$, and over l_∞ linearily decreases. This decrease is expressed the stronger, the thicker the fibre is. In the gravitational spinning A 5 σ falls to zero at $x = L$; in an extreme case of infinitely thin fibre it would be constant above $x = l_\infty$.

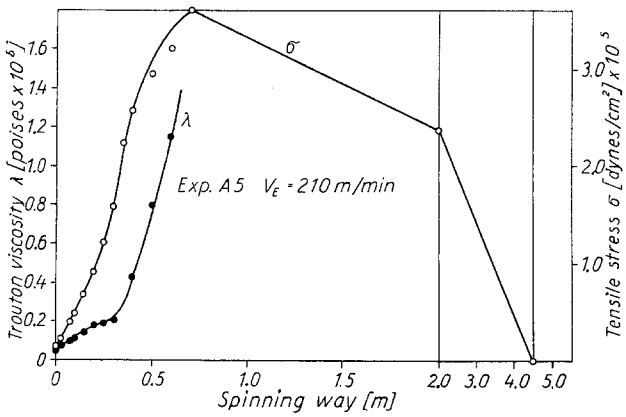

Fig. 10. Distribution of stress and apparent *Trouton* viscosity along the spinning way. Experiment No. A5

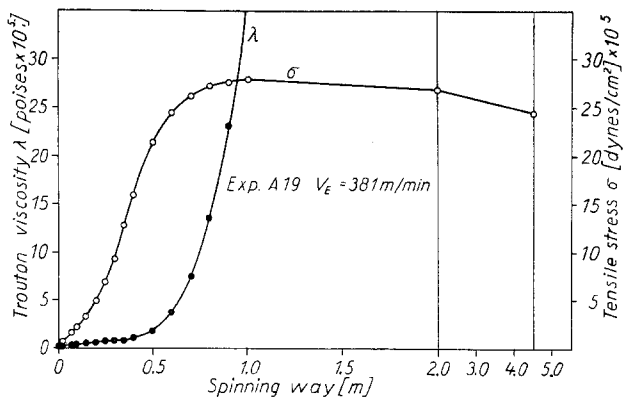

Fig. 11. Distribution of stress and apparent *Trouton* viscosity along the spinning way. Experiment No. A19

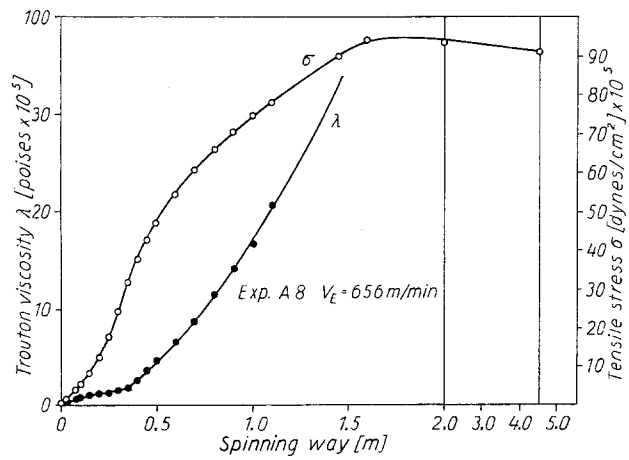

Fig. 12. Distribution of stress and apparent *Trouton* viscosity along the spinning way. Experiment No. A8

It is characteristical for each experiment, that the viscosity variation shows a distinct turn at the distance l_c = 30–35 cm. On this distance a maximum of velocity gradient G was always observed (1). This is an evidence for previously expressed suggestion concerning the transition effects in polymer in this point. All the viscosity-spinning way characteristics are monotonically increasing curves. This increase, postulated in theoretical considerations (1) is a fundamental principle of fibre spinning process.

The effect of spinning conditions upon the take-up force, gravitational force and stress

As comparative characteristics for the force constituents in a given spinning experiment, the maximal values at $x = 0$ were calculated.

The gravitational force F_{grav} was calculated with a simplification, assuming the fibre on the whole way to have constant, final thickness (Td deniers). Hence, for L = 450 cm:

$$F_{\text{grav},0} \approx 0{,}5\, Td \text{ (dynes)}.$$

A similar assumption was taken for aerodynamical force, which was calculated for L = 450 cm and the final velocity V_E, according to formula:

$$F_{\text{aero},0} \approx 0{,}0212\, W^{0.5}\, V_E .$$

The inertial force F_{inert} in the distance $x = 0$ amounts to:

$$F_{\text{inert},0} = W\,(V_E - V_0)$$

and the rheological constituent resulted from the balance of the residual constituents including F_{ext}:

$$F_{\text{rheo},0} = F_{\text{ext}} + F_{\text{grav},0} - F_{\text{aero},0} - F_{\text{inert},0} .$$

In each diagram there are three functions given:

1. the total drawing force (sum of positive constituents):

$$F_{\text{tot}} = F_{\text{ext}} + F_{\text{grav},0} .$$

2. the rheological force $F_{\text{rheo},0}$

3. the maximal stress $\sigma_{\max}$ calculated on the final cross-section:

$$\sigma_{\max} = F_{\text{rheo},0}/A_{x=l_\infty} .$$

Effect of take-up velocity V_E at constant intensity of flow: W = const.

An increase of take-up velocity V_E at W = const. and variable fibre thickness is accompanied by nearly linear increase of F_{tot} and F_{rheo} (fig. 13). The increase of velocity is here combined with an increase of the rate of cooling due to the increasing ratio: fibre surface/fibre volume. Such changes lead to a decrease of the

gravitational constituent in the total drawing force from 13.8% at V_E = 332 m/min and Td = 78.6 drs to 0.3% at V_E = 2860 m/min and Td = 9.13 drs.

Since all the negative constituents (drags) increase nearly linearily with V_E, the rheological force is also a linear function of velocity and amounts to 82 ± 2% of the sum of drags.

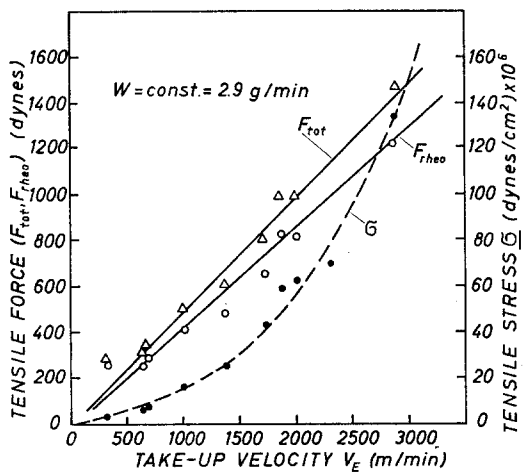

Fig. 13. Dependence of total drawing force, rheological force and stress on the take-up velocity at constant intensity of flow W = 2.9 g/min

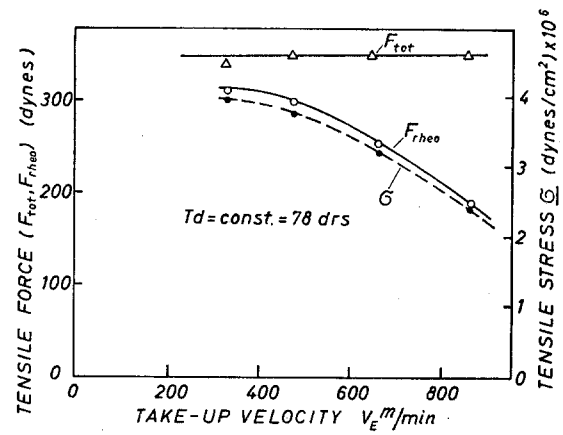

Fig. 14. Dependence of total drawing force, rheological force and stress on the take-up velocity at constant fibre thickness Td = 78 drs

The stress increase is more rapid than linear against V_E. This is a result of two equally directed effects: an increase of velocity gradient and an increase of cooling rate, as mentioned above.

Effect of take-up velocity V_E at constant fibre thickness: Td = const.

The change of take-up velocity at constant fibre thickness and variable intensity of flow leads to quite other effects. The total drawing force and naturally the fibre cross-section remain constant, while the rheological force and stress decrease with V_E (fig. 14).

From the analysis of individual constituents it may be seen, that the inertial and aerodynamical forces increase from 9% sum of drags at V_E = 364 m/min and W = 3.15 g/min to 46% at V_E = 862 m/min and W = 7.55 g/min. The corresponding decrease of rheological force is given respectively by 91% sum of drags at V_E = 364 m/min and 54% at V_E = 862 m/min.

An increase of velocity at constant fibre thickness is combined, as a rule, with a decrease of cooling rate and an increase of average fibre (stream) temperature. The observed decrease of stress is a result of two opposite effects: an increase of velocity gradient, and a decrease of average viscosity.

Effect of fibre thickness Td at constant take-up velocity: V_E = const.

The change of fibre thickness (titre-deniers, Td) and naturally its diameter d was accomplished by increasing the number of dies n in the spinneret at constant intensity of flow W. The increase of number of filaments n is connected with an increase of cooling rate and average viscosity of stream.

As is could be expected, an increase of n brought about an increase of total- and rheological force as well as an increase of stress (see fig. 15).

Simultaneously increased the part of rheological force in the sum of drags from 72.6% at n = 1 and Td = 67.6 drs to 96.3% at n = 12 and Td = 5.64 drs. In view of the above said, such a behaviour seems to be quite obvious.

The effect of cooling conditions was investigated also by changing the conditions of air flow in the leading tube. Two spinning experiments were carried out at constant take-up velocity, flow intensity and fibre thickness:

1. with leading tube closed in its lower end and practically immobile air within the tube;
2. with leading tube open in the lower end, and a natural air draught of about 1–2 m/sec speed.

The results for two sets of spinning conditions are shown in table 1.

Table 1

Take-up force F_{ext} (dynes) for various cooling conditions

A: monofilament yarn $Td = 50$ drs; $V_E = 720$ m/min
B: multifilament yarn $Td = 120/12$ drs; $V_E = 866$ m/min

	A	B
1. Leading tube closed, immobile air	400	4900
2. Leading tube open, natural air draught	610	5400

It is evident, that an intensification of cooling, arising from an air draught, leads to an increase of take-up force F_{ext}. Similar effects have been also observed in fibre birefringence (9).

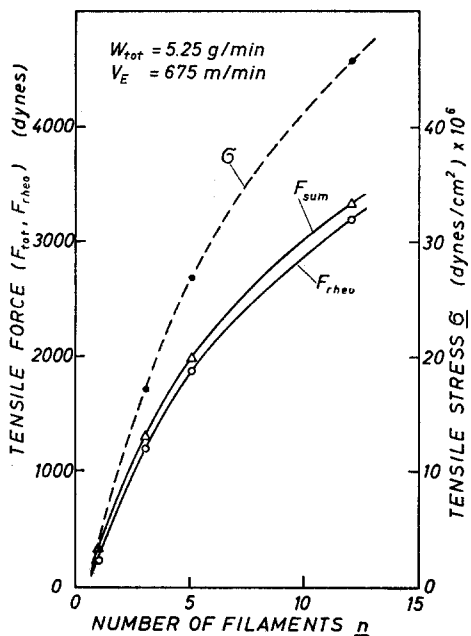

Fig. 15. Dependence of total drawing force, rheological force and stress on the number of filaments, at constant total intensity of flow $W = 5.25$ g min and take-up velocity $V_E = 675$ m/min

The effect of the diameter of spinneret channel d_0 was not observed, when monofilaments of constant thickness and at constant take-up velocity were spun. The take up force oscillated about some average value. This behaviour seems to be clear, since it was formerly found that the diameter d_0 affects but slightly the initial part of the stream. The slight changes of F_{grav} and F_{aero} were not detected by our experiments.

Effect of friction of fibre on the wetting device

All the force data discussed above were obtained from the measurements in which the fibre ran freely between the spinneret and the winding drum. Such a system of experiments was marked in fig. 7 as "position *a*".

In technical conditions the fibre is, as a rule, led through a wetting device, consisting e. g. of a wetting disc (W) and leading roll (R) (fig. 7). In order to establish the effect of friction on those elements, the force measurements were carried out in 3 systems:

1. free running fibre, without wetting (fig. 7 pos. "*a*");
2. fibre wetted by a tangential contact with the wetting disc W but without leading through the roll R;
3. fibre led through the leading roll R and the wetting disc W as in technical practice (fig. 7 pos. "*b*").

Fig. 16. Tensiometric curves for various systems of fibre leading. 1. – freely running fibre; 2. – fibre tangentially wetted; 3. – fibre led through the leading roll and the wetting disc. (cf. table 2, yarn B)

The results are shown in the table 2 and in fig. 16.

Table 2

Take-up force F_{ext} (dynes) for various systems of fibre leading

A: monofilament yarn $Td = 70$ drs, $V_E = 477$ m/min
B: multifilament yarn $Td = 70/12$ drs; $V_E = 675$ m/min

	A	B
1. Freely running fibre	312	3375
2. Fibre wetted tangentially	1113	4750
3. Fibre led through the roll R and the disc W	1500	8750

It is clearly evident that the forces measured with included wetting device are several

times greater than those found for freely running fibre. Moreover, the inclusion of wetting device leads to an increase of the amplitude of oscillation (see fig. 16). The stress between the elements of wetting device and the winding drum, though greater than the tensile stress σ between the spinneret and the leading roll, seems to have no influence upon the spinning process. In this region fibre should be solid and not undergo an irreversible deformation. The force measurements, however, carried out with included wetting device are incompetent for the conditions of fibre formation. All the force measurements which are thought to characterize the spinning process must be always carried out on a free running fibre without wetting and any other mechanical drags.

The above described relations between the spinning conditions and the tensile stress σ are somewhat similar to those found for spinning conditions and the fibre birefringence (7). The birefringence, like stress, increases with take-up velocity at W = const. For polycapronamide the relation: Δn vs. V_E is a saturation curve, while the relation σ vs. V_E is a concave one. An increase of number of filaments at W = const., V_E = const. leads to an increase of birefringence as well as of stress. A different behaviour occurs by the effect of velocity V_E at constant fibre thickness. In the investigated range of variables, the stress was found to decrease with V_E, while birefringence increased with velocity. Hence the conclusion, suggested in previous works (9) that the tensile stress is more sensitive to the cooling conditions than to the rate of deformation. The birefringence shows an opposite behaviour. The explanation of the mechanism of that phenomenon requires, however, more extensive theoretical and experimental studies.

Some correlation between the degree of orientation (birefringence) and the tensile stress, or take-up force, makes it possible to apply the simple and continuous tensiometric measurements to the observations and control of the spinning process in practice. The force F_{ext} is sensitive as well to the oscillations of take-up velocity as to the hard-measurable changes in cooling conditions, polymer viscosity fluctuations etc. In any way the continuous measurements of take-up force F_{ext} will allow to compare the work of various spinning machines and to find the origins of some disturbances in the technological process.

Conclusions

The theoretical analysis of mechanical effects occurring by fibre spinning process has shown that this process can be approximately treated as a motion of liquid in which the tensor of velocity consists of x-constituents only, and the velocity gradient in the directions of y and z is zero:

$$V = \begin{Bmatrix} V_{xx}, & 0, & 0 \\ 0, & 0, & 0 \\ 0, & 0, & 0 \end{Bmatrix}$$

In the discussion of possible origins of the appearing of transverse velocity gradients it was shown that the initially parabolic velocity profile in the channel of spinneret will be equalized in a short distance from spinneret, near the zone of stream broadening. Some small surface forces (aerodynamical drag, surface tension) practically do not affect the velocity distribution. The substantial factor, which should be taken into account is a radial viscosity gradient arising in "melt-spinning" from a temperature gradient, in "dry-spinning" from a concentration gradient, and in a "wet-spinning" from the heterogeneous diffusion processes (gelation, precipitation).

Fibre spinning is a peculiar physical process in which takes place a continuous transition of the flow of a liquid stream in the running of a solid fibre. This feature is common for all spinning procedures while in each one there is another physical origin of this transition:

the cooling and solidification of polymer melt in the "melt-spinning", solvent evaporation in the "dry-spinning", and the gelation and precipitation of polymer in the "wet-spinning" procedure. The main processes connected with fibre formation proceed in the liquid stream. The transition into solid, however, leads to some special features. In the solid polymer the distribution of velocity through fibre cross-section is naturally uniform. In the initial part of liquid polymer stream, the distribution of velocity is uniform too, when the effects of spinneret channel are equalized. Hence, as a consequence of the principle of continuity, in any transverse stream cross-section will occur a uniform distribution of velocity.

At such conditions, the radial viscosity gradient leads not to an appearance of radial velocity gradient, but to the corresponding stress distribution. As a result of it, appears in the final fibre a non-uniform radial distribution of the degree of orientation, in

some cases combined with so-called "skin-effects".

The theoretical analysis of force constituents and the experimental data obtained from polycapronamide led to an estimation of the relative importance of various factors in spinning conditions. Some analogies between the tensile stress and fibre birefringence threw a little light upon the mechanism of structural processes.

The experimentally determined distribution of *Trouton* viscosity along the spinning way confirmed our former assumptions about the significance of maxima in the velocity gradient distributions. All the curves: viscosity vs. spinning way are monotonically increasing and show a distinct turn in the point corresponding to the maximum of velocity gradient.

Acknowledgement

The author wishes to express his gratitude to Mrs. *R. Takserman* for many helpful discussions held during the writing of this paper.

Summary

The general theoretical analysis of mechanical effects in the fibre spinning process based upon hydrodynamics has been given. The possibilities of an occuring of radial velocity gradient, and effects connected with the radial viscosity distribution have been discussed. The tensile force and its constituents: the external take-up force, gravitational force, aerodynamical drag, surface tension, and inertial constituent have been analyzed and discussed.

For melt-spun polyamide fibres the direct measurements of take-up force have been carried out and calculated the distributions of stress and viscosity along the spinning way.

The effects of take-up velocity, fibre thickness, cooling intensity and friction on the wetting device upon the take-up force, rheological force and stress have been investigated and discussed.

Zusammenfassung

Eine allgemeine theoretische Analyse der mechanischen Effekte beim Faserspinnprozeß, begründet auf die Hydrodynamik, wird gegeben. Die Möglichkeit des Auftretens radialer Geschwindigkeitsgradienten und die Effekte, verbunden mit der radialen Viskositätsverteilung, werden diskutiert. Die Zugspannung und ihre Anteile: die äußere Abzugskraft, die Schwerkraft, aerodynamische Reibung, Oberflächenspannung und Trägheitswirkung werden analysiert und diskutiert.

Für Polyamidfasern nach dem Schmelzspinnverfahren wurden direkte Messungen der Abzugskraft ausgeführt und die Verteilung von Spannung und Viskosität längs des Spinnweges berechnet.

Die Effekte von Abzugsgeschwindigkeit, Faserdicke, Abkühlung und Reibung an der Befeuchtungseinrichtung auf die Abzugskraft, die Fließkraft und die Spannung werden untersucht und diskutiert.

References

1) *Ziabicki, A.* and *K. Kędzierska*, Kolloid-Z. **171**, 51 (1960).

2) *Ziabicki, A.* and *K. Kędzierska*, ibid. **171**, 111 (1960).

3) *Prandtl, L.*, Führer durch die Strömungslehre (Braunschweig 1949).

6) *Ziabicki, A.* and *K. Kędzierska*, Chem. Stosowana (Wrocław) **1960**, No. 2, 151.

7) *Ziabicki, A.* and *K. Kędzierska*, J. Appl. Polymer Sci. **2**, 14 (1959).

8) *Ziabicki, A.*, ibid. **2**, 24 (1959).

9) *Ziabicki, A.*, Dissertation (Łódź 1959).

From Department of Physics, Faculty of Science, Kyushu University, and Department of Applied Chemistry, Faculty of Engineering, Kyushu University, Fukuoka (Japan)

Note on the Dielectric Relaxation Distribution Function in High Polymers

By Kaoru Yamafuji and Yōichi Ishida

With 2 figures

(Received July 29, 1960)

The shape of the dielectric relaxation time spectrum, $L_\varepsilon(\tau)$, for the solid high polymer seems to have the following distinguishable characteristics compared with the mechanical retardation time spectrum, $L_m(\tau)$:

(1) The gradient of $L_\varepsilon(\tau)$ is, in general, much sharper than that of $L_m(\tau)$ especially for the amorphous polymer. The values of the *Cole*'s parameters, $\bar{\beta}$, for the dielectric dispersions in various polymers are plotted against the temperature in fig. 1, where the $\bar{g}$, the mean gradients of the $\log L_\varepsilon(\tau)$ vs. $\log \tau$ curves corresponding to $\bar{\beta}$, are also plotted on the right hand side. In the amorphous polymers such as polymethylacrylate (PMA), polybutylmethacrylate (PBMA) and polyvinylacetate (PVAc), the values of $\bar{g}$, for the dielectric α-dispersions are nearly equal to 1 or so. These values of $\bar{g}$ are much larger than $^1/_2$, which is known as the value for the mechanical α-dispersion. On the other hand, the values of $\bar{g}$ for the dielectric α-dispersion in the crystalline polymers such as polymonochlorotrifluoro-